

# The Effects of Voids on the Flexural Properties and Failure Mechanisms of Carbon/Epoxy Composites

M. A. Suhot<sup>a</sup>, A. R. Chambers<sup>b,\*</sup>

<sup>a</sup>UTM Razak School of Engineering and Advanced Technology, Universiti Teknologi Malaysia, 54100, UTM Kuala Lumpur Malaysia

<sup>b</sup>School of Engineering Sciences, University of Southampton, Highfield, Southampton SO16 3DU, UK

\*Corresponding author: arc1@soton.ac.uk

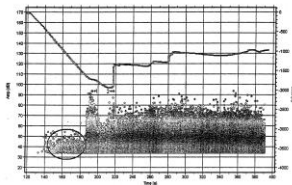
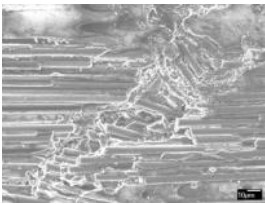
## Article history

Received :19 June 2014

Received in revised form :8 July 2014

Accepted 24 August 2014

## Graphical abstract



## Abstract

Although the effect of voids on the mechanical properties of composite failures has been well researched, their effect on the failure mechanisms has not been well characterised. This study investigated the effect of the void content on the flexural strength of carbon/epoxy composites and to explain in terms of the failure mechanisms. The results showed that a 2% increase in void content reduced the flexural strength by 12.7%. Using optical microscopy, X-ray tomography and acoustic emission it was found that voids had no effect upon compression crack initiation but were found to influence the initiation and propagation of delaminations. A combination of in-situ acoustic emission and X-ray tomography proved to be a powerful tool in providing evidence of the failure mechanisms.

**Keywords:** Voids; flexural strength; carbon fibre; acoustic emission; x-ray CT scan

© 2014 Penerbit UTM Press. All rights reserved.

## 1.0 INTRODUCTION

Although the effect of voids on the mechanical properties of structural polymer fibre composites has been studied for many years, the role of voids in determining the mechanical properties and failure mechanisms of polymer fibre composites is still not fully understood.

It is universally accepted that increasing void levels have an adverse effect on the mechanical properties. Tensile properties of structural composites, which are fibre dominated, are less affected than the compressive and flexural properties which are resin dominated [1]. Frequently, in the literature, the effect of the voids is described in terms of % reduction in property or % void content increase. Although this information is useful, it is clear that there is much variation in the quoted values due to differences in the materials, their architecture and problems in accurately quantifying the void levels. If realistic predictive models are to be developed to predict damage, it is important that the failure micromechanisms and how they are influenced by voids are understood.

There are many studies showing the role of void content in controlling the mechanical behaviour of polymer matrix

composites [2, 3]. However, with the exceptions of the work by Bilger *et al.* [4] and Cheng and Guo [5] studies in quantifying dependencies between void characteristics and the initiation and/or accumulation of damage are very few.

With regard to flexural properties, the adverse effect of voids has been attributed to a number of factors; the decrease of strength due to the presence of voids, including voids acting as a break in fibre-matrix adhesion [6], occurrence of shearing due to the presence of voids in fibre/matrix interface and resin [7], reduction of the cross-sectional area, acting as a failure initiator [8] and a variation of a notched strength criterion [9]. Wisnom *et al.* [10], Jeong [7] (both for unidirectional laminates) and Costa *et al.* [11] (for woven fabric) on the influence of voids on the interlaminar shear strength show that cracks initiate from voids and propagate longitudinally at the interface of the fibre or the matrix.

Studying void effects on the mechanical behaviour of composites is not a simple task. In addition to the void content, void location also has to be considered in analysing the laminate mechanical behaviour. Due to the random distribution of voids in composites, the voids may or may not be positioned in such a way that they cause/influence premature failure. Hence laminates with a similar void content may show a different mechanical

behaviour[6]. The void content and size will determine the extent of decrease in properties as compared with the void free composites. In addition, the distribution of voids can be expected to have a significant effect on the performance, as properties will be decreased locally in the region of a higher void content.

Traditionally, voids have been measured and quantified using optical microscopic techniques. Whilst having the advantage of being able to identify small voids, these techniques suffer the serious disadvantage of not being able to provide spatial distribution or allow the initiation and propagation of damage from voids to be monitored in-situ. Recently, X-ray tomography has been used to study the internal structure of composites. For examples are the works by Awaja *et al.* [12] and Cosmi *et al.* [13]. X-ray tomography showed the advantage of non-destructively characterising the internal structures of composites and other types of materials.

Although much is known about voids, there is still a need for the improved knowledge on the mechanisms influencing failure. Taking all these points into consideration, it is possible to conclude that there is a need to study the effects of voids on mechanical properties. Thus the main objective of this study is to measure the void characteristics and relate them to the material properties and the failure mechanisms.

## 2.0 MATERIALS AND METHODS

In order to achieve an understanding of the role of voids on flexural failure, 4-ply unidirectional laminates in carbon/epoxy with different void levels were manufactured and tested under flexural loading. The effect of voids on the flexural strength was quantified and the sequence of failure mechanisms established using acoustic emission and X-ray tomography.

### 2.1 Materials And Manufacture

Two carbon fibre prepreg materials were used in order to achieve void contents in the range 0.5-8%. Both used 500g/m<sup>2</sup> fibre with an epoxy resin system. The first was SPRINT, a prepreg manufactured by Gurit (Isle of Wight, UK) consisting of a layer of fibre reinforcement on each side of a precast, pre-catalysed resin film, with a light tack film on one face. This is laid up and cured in a similar manner to conventional prepreg. The second was a conventional unidirectional prepreg, WE91 also manufactured by Gurit.

In order to produce different void contents in the four ply SPRINT laminates, four different vacuum pressures; 100% (manufacturer recommended), 90%, 80% and 70% were used in the cure cycle. With the prepreg, void content was varied by either debaulking (panel 8266) or not debaulking (panel 8267) the lay-up stack. All panels were oven cured for one hour at 120°C.

Each panel is then sectioned (refer to Figure 1) using a diamond cutting wheel in order to produce mechanical test pieces and sections for metallographic analysis.

### 2.2 Flexural Testing

The three-point bending test, as established by ASTM Standards D790 [14], consisted of a simply supported beam between two roller supports (radius 4 mm) with the load applied at the midpoint by a roller (6.5 mm radius). The support span-to-depth ratio was  $L:d = 16:1$ , where  $L$  is the distance between the lower fixed rollers and  $d$  is the specimen thickness. The length of the specimen was parallel to the fibre direction. The tests were performed using an Instron 8872 under load control.

Four-point bending tests according to the ASTM D790 Standards were also conducted in order to isolate the three-point bending roller compression influence from any void effect. A similar span to depth ratio (16:1) was used and the distance between the loading noses was one-half of the support spans. Linear displacement was measured using a linear displacement voltage transducer (LVDT) placed directly under the mid-span of the specimen. Apart from the usage of LVDT, the test procedure of the four-point bending test is the same as the three-point bending test.

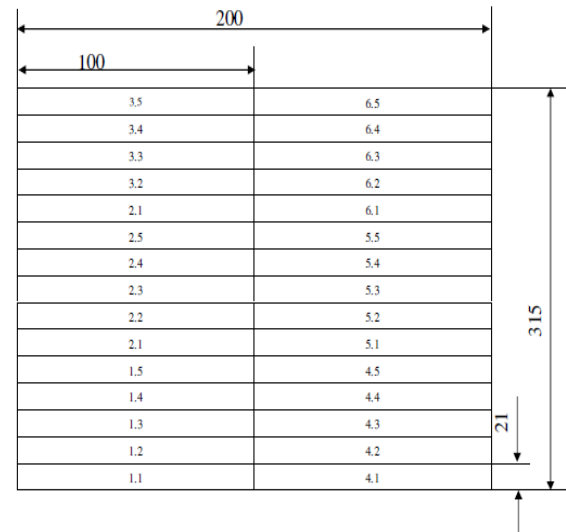


**Figure 1** Layout of panel where fibres run parallel to the horizontal direction. All dimension in millimetres. Specimen number is indicated in the figure

### 2.3 Void Characterisation

Voids were quantified and characterised using image analysis. The specimens for image analysis were carefully prepared using a polishing regime commencing with 120-grade silicon carbide abrasive paper and finishing with 1 µm diamond paste. The image analysis was conducted in the manner of previous work [15] where a magnification of x100 and the analysis of five images per specimen provide a reliable void characterisation. The five images were taken at 4 mm intervals in the transverse direction. The images were captured and saved using XCap image capture and analysed using a tessellation analysis programme. The analysis provided a quantification of void content, void size and shape (aspect ratio). The voids are classified into six different void types depending on their sizes. The classification of these voids is shown in Table 1.

**Table 1** Void type based on size

Void type	Lower size limit (µm <sup>2</sup> )	Upper size limit (µm <sup>2</sup> )
0	0.0	0.9
1	1.0	9.9
2	10	99
3	100	999
4	1000	9999
5	10000	-

## 2.4 Damage Characterisation

A major objective of this study is to relate failure initiation and propagation to the presence of voids. X-ray tomography allows visualisation of the damage in 3D without damage to the specimen hence it was possible to monitor damage initiation and progression during loading.

The X-ray micro CT images are acquired using the X-TEK Benchtop CT 160Xi machine. It is a benchtop type machine which has a resolution down to 5  $\mu\text{m}$  focal spot reflection target and an X-ray source which operates at 25-160 kV and 0-1000  $\mu\text{A}$ . The scans in this study were carried out with the X-rays at a voltage of 45 kV and a current of 100  $\mu\text{A}$ . The 3D reconstruction was performed using X-TEK reconstruction software and visualisation and the analysis carried out by using a commercial software package 'VGStudiomax 1.2' (Volume Graphics GmbH, Heidelberg, Germany).

## 2.5 Acoustic Emission (AE)

The acoustic emission sensor (PicoZ Broadband, diameter = 3 mm) was glued to the bottom of the three-point bending and four-point bending specimens. Only one sensor was used because the location of the crack is always located at the bottom of the roller. The sensor was connected to the preamplifier with 110 kHz high pass and 1MHz low pass filters. The preamplifier was then connected to the amplifier. The amplifier was also connected to the load and position readings of the Instron machine. The AE data was analyzed using Vallen AE software. The software is set using 3.33 MHz sample rate, 34 dB threshold and 40 dB gain. For each test, the AE data acquisition was started at the same time as the loading. The parameter-based analysis was used in the processing of the AE data, where the amplitude and the energy were the main AE characteristics being analyzed.

## 3.0 RESULTS AND DISCUSSIONS

Most interestingly, the ratio of the two components has a profound effect on the microscopic structure and macroscopic properties of the gel in toluene.

### 3.1 Void Characterisation

Samples from all the materials were assessed for quality prior to flexural testing using image analysis. The results are presented both in terms of total void content and the proportion of voids within specific size ranges.

From Figure 2, it can be seen that debaulking the prepreg significantly reduced the total void content primarily as a result of reducing the number of larger voids (area  $>10000 \mu\text{m}^2$ ). With SPRINT, improving the quality of the vacuum resulted in a similar but less dramatic effect. Even with low average void panels, significant local variation in void content was found.

Aspect ratio was also characterised and no significant difference was found between any of the materials. Approximately 80% of the voids had an aspect ratio between 1 and 2, with the remainder being between 2 and 4. For this reason, aspect ratio is not considered to be a major factor in contributing to any of the differences in the mechanical test results.

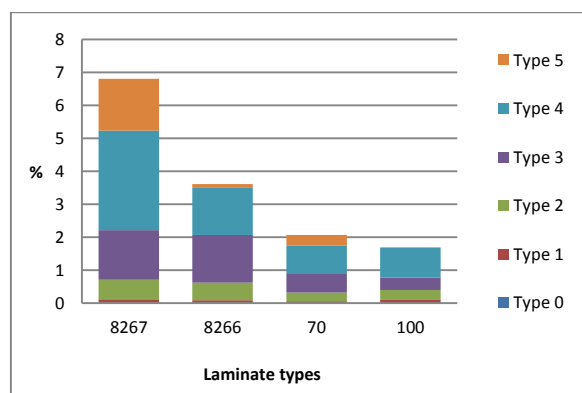


Figure 2 The percentage of void area for each type of void

### 3.2 The Effect Of Voids On Flexural Strength

Given the variability in void contents and distribution of voids within a laminate, all void content measurements presented in this research were taken 30 mm from the failure area. The results of flexural strength as a function of the average void content are presented in Figure 3. From the trend line, it is apparent that an increase of 2% of voids resulted in the decrease of flexural strength by 12.7%. The reduction in flexural strength due to increasing void content was 13.8% for every 2% increase in the void content and is similar to the value quoted by Liu *et al.* [16]. In Ghiorse's [1] study, using woven material, however, the drop-off rate for the cross-ply laminate was 20% for every 2% increase in the void content which illustrates the dependency on material composition and architecture.

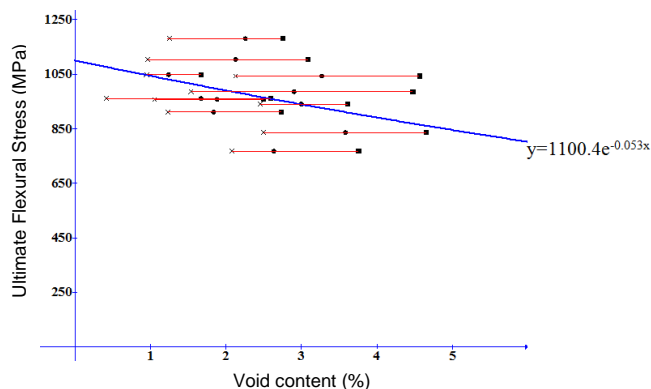
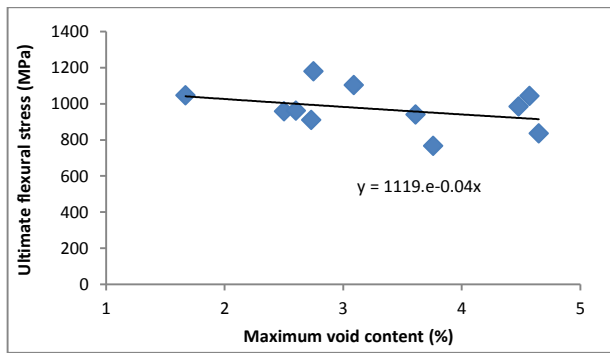


Figure 3 The ultimate flexural stress vs. the void content for SPRINT

The relationship between the maximum void content and the ultimate flexural stress is shown in Figure 4. The equation of the trend lines for average and maximum void contents are in close agreement which suggests that void effects are determined more by large voids than small voids and that presenting void effects in terms of void size ranges may be as revealing as using average void content.



**Figure 4** The ultimate flexural stress vs. the maximum void content for SPRINT materials

**3.3 The Microscopic Mechanisms Of The Three-Point Bending Test Failure**

Irrespective of the void content, the basic mechanism of failure remained the same. A typical failure observed visually is characterised by the initiation and propagation of a crack on the compression side directly underneath the roller followed by a series of delaminations.

Optical microscopy and SEM analysis of samples loaded up to 40% and 80% of the mean expected failure load revealed no evidence of the formation of a crack underneath the roller or obvious changes in the microstructure. At these loads the samples were still below the first load drop shown in Figures 11 & 12 as shown in Section 3.5 (Acoustic Emission). SEM of tests halted at the first load drop revealed the presence of the compression crack beneath the roller (Figure 5a).

Optical microscopy of the compression crack showed both fibre fracture and kinking (Figure 5b). After the initial load drop, the load increased again until a maximum at which a series of delaminations resulted in progressive load reduction until failure.

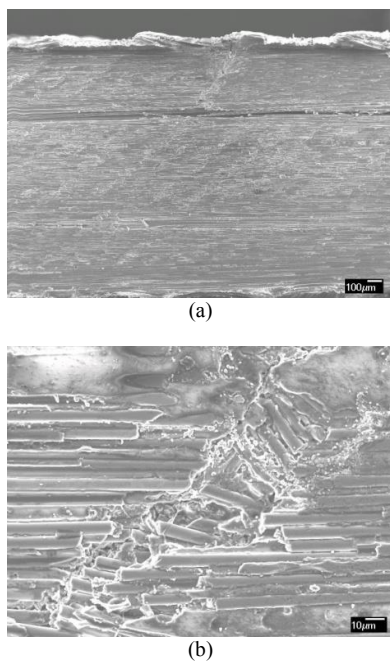


**Figure 5** The failure of the three-point bending specimen showing compressive damage from under the roller, propagating towards the middle of the specimen and the delamination starting from the crack

**3.4 The Effect Of Voids On The Failure Mechanism**

The flexural test results clearly showed that the flexural strength reduced as the void content increased. Further X-ray tomography and optical analysis was conducted in order to establish the effect of voids on the failure mechanism.

The first stage of failure was the formation of a compression crack. In all the examples examined, no void was observed in the compression crack. The second stage involved delamination and here voids were found to play a role both in delamination initiation and propagation. In Figure 6a, the compression crack can be seen to be deflecting to a large void and in Figure 6b a delamination has initiated at a void.

When observing large samples, the resolution of the CT scan is reduced and it is not possible to isolate individual fibres and small voids. Hence destructive microscopy was performed on the samples loaded to 40 and 80% of failure to identify damage and the role of voids prior to the first load drop and prior to the formation of the compression crack. Image analysis on samples cured less than 1 atmosphere vacuum revealed that the void content increased from 1.5 to 3.4% as the load was increased from 40 to 80% of the expected failure load. This may be an indication of small voids growing and coalescing in the early stages of loading. Figure 7 of a failed samples show that the growth of coarse cracks in the resin rich region has been influenced by pre-existing voids.

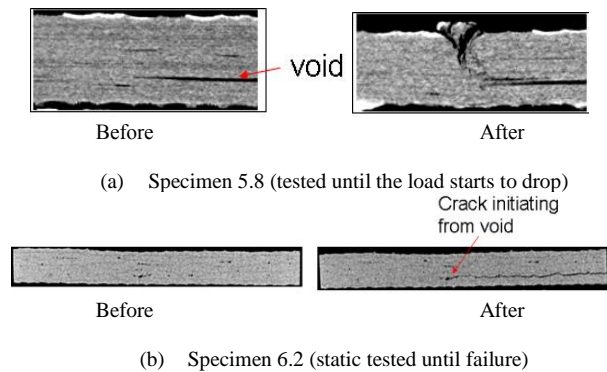


**Figure 6** The X-ray tomography images before and after loading in the static test

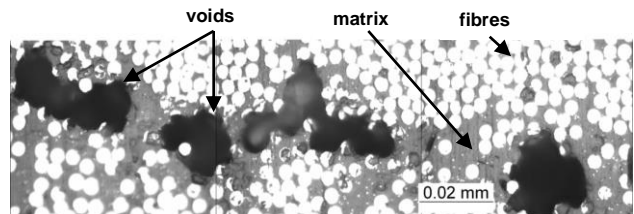


**Figure 7** A higher magnification of the loaded 70% vacuum specimens

**3.5 Acoustic Emission And Failure Mechanism**

Acoustic emission was used to further the understanding of the mechanism of the static failure of CFRP. Three-point bending test with the acoustic emission data acquisition equipment was performed on two different qualities of the unidirectional composites. The average void content based on 15 measurements was 1.95% for the low void content material and 9.04% for the high void content material.

Figures 8 and 9 show energy plotted against the event duration for high and low quality specimens. A comparison of Figures 8 and 9 shows that the failure mechanisms of the low and high void specimens cause different energy responses. The high void content specimen demonstrated many low energy-high duration events (circled in Figure 8) compared with the low void material whilst the low void material exhibited more high energy long duration events (circled in Figure 9).

Siron and Tsuda [17] classify an event with the duration above 10,000  $\mu\text{s}$  as being consistent with delamination. This is in agreement with this study where the final event for the low void content specimen (shown in Figure 9) was delamination.

Further information regarding the failure mechanism is obtained by analysing the amplitude of the events. Figure 10 shows the load curve and the occurring amplitude of each event (displayed as dots) plotted against time. At the section where the load is increasing uniformly, there are only low amplitude events which are consistent with matrix cracking and the fibre/matrix debonding. The high amplitude events can be seen to correspond to a load drop which is probably the formation of the compression crack and is consistent with the X-ray tomography findings. The acoustic emission characteristics of the fibre breakage event consist of high amplitude, a high duration and a low rise time. Event 1 shows this characteristic, where the rise time is 8.4  $\mu\text{s}$  and the duration of 1935.2  $\mu\text{s}$  which can be assumed as a fibre breakage event.

After the initial fibre breakage, the load continues to increase to its maximum and after which a sudden huge drop of load occurs. Event 2 has a rise time of 0.2  $\mu\text{s}$  and the duration of 26483.2  $\mu\text{s}$  which clearly suggests the occurrence of fibre breakage.

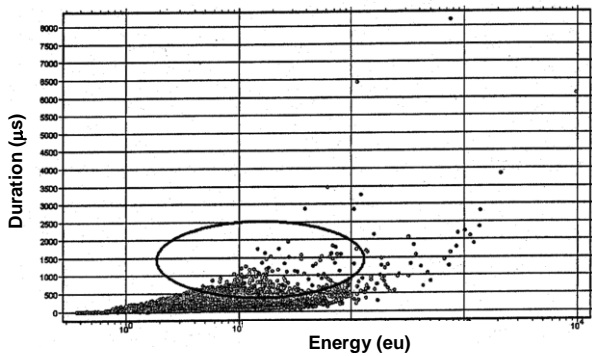


Figure 8 The duration vs. the energy for a high void content specimen

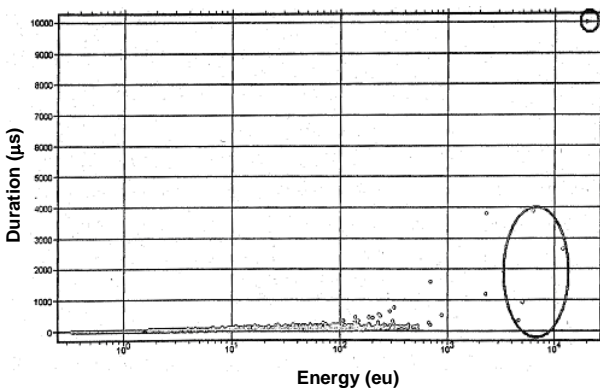


Figure 9 The duration vs. the energy for a low void content specimen

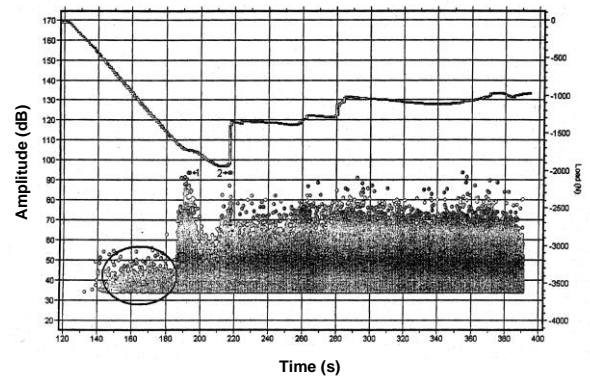


Figure 10 The amplitude vs. time vs. the load graph for a low void content specimen

Such similar failure mechanisms can be seen to occur from the AE data in a high void content specimen in Figure 11. The initial drop in load corresponds to the events with low rise time and long durations which is indicative of fibre breakage. It is rather unusual for the event corresponding to the load drop after maximum load (Event 1 in Figure 11) to be of low amplitude. But the event is of a long duration, with a low rise time and with high energy which confirms that failure is caused by the fibre breakage.

The amplitude versus time results of the low and high void content show a similar pattern of behaviour. However, in studying the acoustic energy event, it is observed that significant differences exist between the low and high void content specimens. For the low void content specimens, the high energy events occur during a drop in the load as shown in Figure 12 (high energy events are circled in the figure). Low energy events occur throughout the test. The high energy event is fibre breakage while the low energy events are fibre/matrix debonding and matrix cracking. The high void content specimens show different behaviour in the energy versus time graph (shown in Figure 13). The energy released during the failure event is lower in the high void content specimens as compared to the ones with the low void content.

From the analysis of the acoustic emission events, the failure mechanisms can be determined. It is found that the high void content specimens fail by low energy events which are attributed to the cracking of the matrix and fibre/matrix debonding, while the low void content specimens are able to sustain high stress and fail under high energy events which are associated with fibre breakage. This shows that the presence of voids affect more matrix cracking and fibre/matrix debonding than fibre breakage.

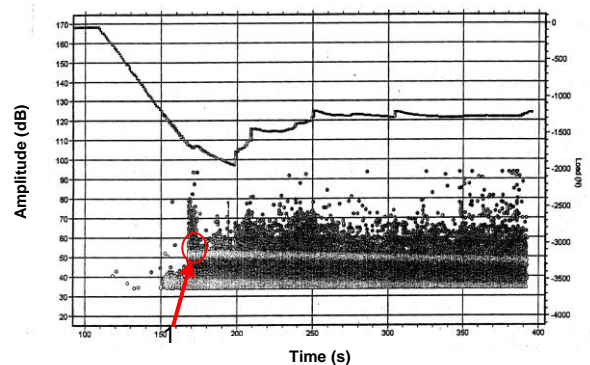


Figure 11 The amplitude vs. time vs. the load graph for a high void content specimen

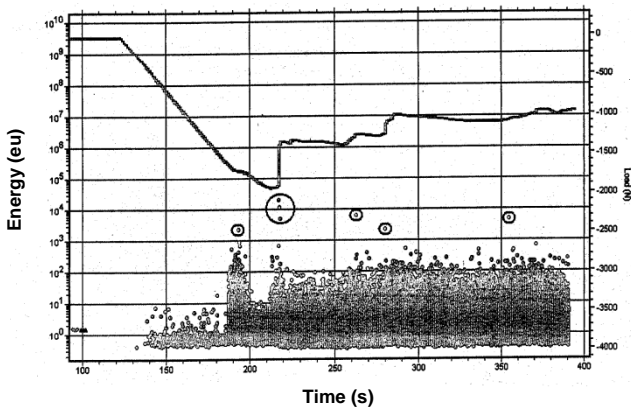


Figure 12 Energy vs. time vs. the load graph for a low void content specimen

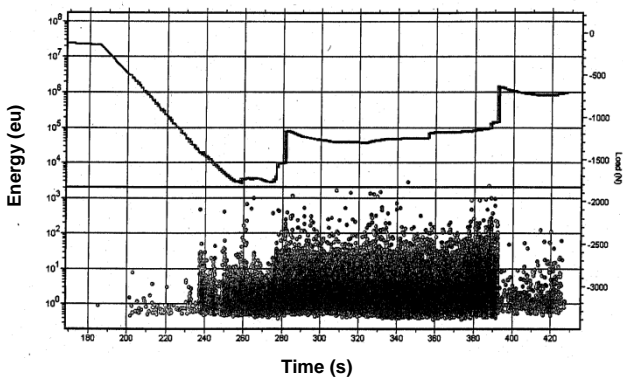


Figure 13 Energy vs. time vs. the load graph for a high void content specimen

3.6 The Four-Point Bending Static Results

The results for three and four-point static bending for prepreg laminates are summarised in Table 2. It can be seen that the strength measured is dependent on both the type of bending and the quality of the material. The flexural strength under the four-point bending is approximately 20% higher than that of three-point bending for both qualities of materials.

It can also be seen that the increase in void content has decreased the average flexural strength in both three and four-point bending. The rate of strength reduction between the three-point bending and the four-point bending calculated from Table 2 is similar. For a 3.2% increase in the void content, the flexural strength from the three-point bending decreased by 19.2% while for the four-point bending, it decreased by 14.2%. Although voids clearly play a role in determining the flexural strength in both three and four-point bending, the results suggest that their influence is not on the formation of the three-point bending compression crack.

Table 2 Three-and four-point bending static test results

Void content (%)	Flexural Stress (MPa)	
	Three-point bending	Four-point bending
3.6	912	1142
6.8	737	979

The static bending test results showed that the static flexural strength reduced by 12.7 % for a 2% increase in the void content. As previously considered, this is consistent with the findings of Liu et al. [16] who also reported similar reductions in both the interlaminar and compressive properties. In this research, the influence of void content on the scatter in the flexural strength results was also considered and it was found that the flexural strength reduced with reducing panel quality. This suggests other void characteristics such as shape, size and distribution may be influencing the results [1].

The evidence provided by the optical microscopic analysis and micro CT scan has demonstrated that the static three point bend failure mechanism involves two stages:

- the formation of a compression crack beneath the roller
- interlaminar cracks and final delamination resulting from the growth of the compression crack.

Clearly, voids have the potential to influence both of these stages. From the load deflection curves of the tests in which the load was removed at varying percentages of the anticipated failure load, it was concluded that the compression crack initiated and developed rapidly in the later stages of loading through a propagation mechanism which, depending on the void content, may involve void coalescence. This is consistent with the results from the AE tests which did not reveal any major events at loads significantly below that of the maximum failure load. The AE demonstrated differences between the low and high void samples in that the low void samples had a much smaller number of low energy events but a greater number of high energy events. This suggests differences in the failure mechanisms and on this basis it is suggested that the low energy events are associated with matrix crack propagation whereas the high energy events are more associated with fibre fracture and delaminations. This argument is consistent with the evidence supplied by the optical microscopy. It should be noted that the filtering of the AE response to remove background testing noise may have taken out low level AE responses from the early damage mechanisms such as microcracking which was observed using optical microscopy.

There are a number of factors which can affect both the formation of a compression crack and the initiation and the propagation of delaminations. These include fibre alignment and voids. Fibre alignment was not a focus of this research and every effort was made in panel manufacture to avoid it. No evidence was found from optical microscopy, CT scan, acoustic emission or the comparison of three and four point test results to suggest that voids affected the compression damage. Hence it is hypothesised that voids do not directly affect the failure through promoting compression damage.

The microscopic analysis has provided evidence to support this hypothesis in that it was shown that voids act as an easy crack path and contributed to matrix cracking and fibre/matrix debonding. It was found consistently, that the major voids were located in the resin rich regions between the plies and where the delaminations occurred. This highlights a problem with the void analysis in this research in that it failed to take into account the importance of void location. Future work should address this and try to take into account the location and distribution of voids.

X-ray tomography also proved useful in determining the role of voids in the failure process. It was found that cracks could initiate at voids and propagate through them and confirmed the findings of the optical microscopy. This was not always the case and depended on the void location. The X-ray tomography work was limited by the resolution of the equipment and therefore the above comments apply to large voids only. It is not possible to make further deductions from this work for this reason.

AE also revealed differences in the failure processes of low and high void content specimens. With the low void content specimens the number of low energy events was lower than with the high void samples.

#### ■4.0 CONCLUSIONS

- It was found that a 2% increase in void content reduced the flexural strength by 12.7%. It was considered that void size is an important void characteristic.
- Voids had no effect upon the initiation of a three-point bend compression crack but played a major role in the initiation and propagation of delaminations.
- A combination of in-situ acoustic emission and X-ray tomography is a powerful tool in the investigation of failure mechanisms.

#### References

- [1] S.R. Ghiorse. 1993. 'Effect of void content on the mechanical properties of carbon/epoxy laminates'. *SAMPE Quarterly*. 24: 54–59.
- [2] J. Muric-Nesic, P. Compston, Z.H. Stachurski. 2011. On the void reduction mechanisms in vibration assisted consolidation of fibre reinforced polymer composites. *Compos. Part A-Appl. S.* 42: 320–327.
- [3] J.Y. Park, A.H. Zureick. 2005. Effect of filler and void content on mechanical properties of pultruded composite materials under shear loading. *Polym. Composite*. 26(2): 181–192.
- [4] N. Bilger, F. Auslender, M. Bornert, H. Moulinec, A. Zaoui. 2007. Bounds and estimates for the effective yield surface of porous media with a uniform or a nonuniform distribution of voids. *Eur. J. Mech A-Solid*. 26: 810–836.
- [5] L. Cheng, T.F. Guo. 2007. Void interaction and coalescence in polymeric materials. *Int. J. Solids Struct.* 44: 1787–1808.
- [6] P. Olivier, J.P. Cottu, B. Ferret. 1995. Effects of cure cycle pressure and voids on some mechanical properties of carbon/epoxy laminates. *Composites*. 26: 509–515.
- [7] H. Jeong. 1997. Effects of voids on the mechanical strength and ultrasonic attenuation of laminated composites. *J. Compos. Mater.* 31: 276–292.
- [8] S.N. Kukureka, C.Y. Wei. 2003. Damage development in pultruded composites for optical telecommunications cables under tensile and flexural fatigue. *Compos. Sci. Technol.* 63: 175–1804.
- [9] S.F.M. Almeida, Z.S.N. Neto. 1994. Effect of void content on the strength of composite laminates. *Compos. Struct.* 28: 139–148.
- [10] M.R. Wisnom, T. Reynolds, N. Gwilliam. 1996. Reduction in interlaminar shear strength by discrete and distributed voids. *Compos. Sci. Technol.* 56: 93–101.
- [11] M.L. Costa, S.F.M. Almeida, M.C. Rezende. 2001. The influence of porosity on the interlaminar shear strength of carbon/epoxy and carbon/bismaleimide fabric laminates'. *Compos. Sci. Technol.* 61: 2101–2108.
- [12] F. Awaja, M.T. Nguyen, S. Zhang, B. Arhatar. 2011. The investigation of inner structural damage of UV and heat degraded polymer composites using X-ray micro CT. *Compos. Part A-Appl. S.* 42(4): 408–418.
- [13] F. Cosmi, A. Bernasconi, N. Sodini. 2011. Phase contrast micro-tomography and morphological analysis of a short carbon fibre reinforced polyamide'. *Compos. Sci. Technol.* 71(1): 23–30.
- [14] ASTM D790. 1990. Standard test methods for flexural properties of unreinforced and reinforced plastics and electrical insulating materials (metric). Philadelphia, PA. American Society for Testing and Materials.
- [15] A.R. Chambers, J.S. Earl, C.A. Squires C.M.A. Suhot. 2006. The effect of voids on the flexural fatigue performance of unidirectional carbon fibre composites developed for wind turbine applications. *Int. J. Fatigue*. 28: 1389–1398.
- [16] L. Liu, B. Zhang, D. Wang, Z. Wu. 2006. Effects of cure cycles on void content and mechanical properties of composite laminates. *Compos. Struct.* 73: 303–309.
- [17] O. Siron, H. Tsuda. 2000. Acoustic emission in carbon fibre-reinforced plastic material. *Annales de Chimie Science des Materiaux*. 25: 533–537.